Chemical Science

EDGE ARTICLE

View Article Online
View Journal | View Issue

Cite this: *Chem. Sci.*, 2017, **8**, 1062

Protecting microRNAs from RNase degradation with steric DNA nanostructures†

H. Qian,[ab] C. Y. Tay,[acd] M. I. Setyawati,[a] S. L. Chia,[a] D. S. Lee[a] and D. T. Leong*[a]

Received 26th April 2016
Accepted 10th September 2016

DOI: 10.1039/c6sc01829g

www.rsc.org/chemicalscience

Tumor suppressive microRNAs are potent molecules that might cure cancer, one day. Despite the many advanced strategies for delivery of these microRNAs to the cell, there are few therapeutic microRNAs in clinical use. Progress in microRNA bioapplications is hindered by a high vulnerability of exogeneous microRNA molecules to RNase degradation that occurs in extra- and intracellular physiological conditions. In this proof-of-concept study, we use a programmable self-assembled DNA nanostructure bearing a "shuriken" shape to not only deliver but more importantly protect a tumor suppressive microRNA-145 for a sufficiently long time to exert its therapeutic effect in human colorectal cancer cells. Our DNA nanostructure harbored complementary sequences that can hybridize with the microRNA cargo. This brings the microRNA–DNA duplex very close to the core structure such that the microRNA cargo becomes sterically shielded from RNase's degradative activity. Our novel DNA nanostructure based protector concept removes the degradative bottleneck that may plague other nucleic acid delivery strategies and presents a new paradigm towards exploiting these microRNAs for anti-cancer therapy.

Introduction

Self-assembled DNA nanostructures hold great potential in the fields of photonics, bioimaging, nanomedicine and biosensing due to their programmable capability from one to three dimensions, their biocompatibility, the readiness of their uptake by cells and their relative stability inside cells. These capabilities have spawned many interesting strategies for designing and constructing structures out of DNA; however, there has not been a deluge of applications arising from these interesting structures. There are pockets of bioapplications of these fascinating structures as nanosized carriers of drugs,[1–5] siRNA,[6,7] peptides[8,9] and in- and out-of-cell sensors.[10–14] This window clearly presents an emerging area for the applications of DNA nanostructures in such fields.

MicroRNA (miRNA) is a class of short RNAs that governs multiple intracellular and extracellular biofunctional processes.[15,16] Amongst this very large family of miRNA, miRNA-145 (miR-145) stands out as a very important therapeutic molecule due to its inherent powerful tumor suppressive effect on cancer. It was reported to be down-regulated in most cancer cell lines and tissues[17] such that reinstating miR-145 could almost immediately suppress tumor growth, and block cell invasion and metastasis.[18] However, while the biological effect is strong, pragmatic issues of delivery, target specificity and successful protection against endogenous nucleases prevent any real progress towards its intended use as a clinically usable therapeutic, as with most miRNA driven anti-cancer therapeutics, which face similar issues. Commercially available specially designed transfection reagents for miRNAs and siRNAs may work well on cell cultured cells but these reagents are typically liposomes of micrometer sizes with a wide size distribution and earlier versions do exhibit some toxicity.[19] Much effort has gone disproportionately into developing better and more advanced delivery strategies[20–24] but this suffers from the law of diminishing returns. In reality, delivery is only the beginning of the journey that each exogeneous miRNA undergoes. Once in the intracellular environment, the exogeneous miRNAs are tagged as foreign and shuttled to the lysosomes[25] where degradation takes place. This degradative process greatly diminishes the actual working concentration of the therapeutic miRNAs and immediately curtails the overall efficacy of the miRNAs, even those delivered at high efficiency. The irony is that ever-increasing delivery efficiency cannot solve the core stability problem. With high delivery efficiency, a high dose with non-specificity will negatively affect the non-targeted non-cancer cells. This lack of tools to protect exogenous miR-145 has prompted the imperfect solution of using plasmid or viral vectors to overexpress miR-145 in cancer cells; this strategy has

[a]*Department of Chemical and Biomolecular Engineering, National University of Singapore, 4 Engineering Drive 4, Singapore 117585, Singapore. E-mail: cheltwd@nus.edu.sg; Fax: +65 6779 1936; Tel: +65 6516 7262*

[b]*Institute of Respiratory Diseases and Critical Care, Xinqiao Hospital of Third Military Medical University, 183 Xinqiao Street, Chongqing 400037, China*

[c]*School of Materials Science and Engineering, Nanyang Technological University, N4.1, Nanyang Avenue, Singapore 639798, Singapore*

[d]*School of Biological Sciences, Nanyang Technological University, 60 Nanyang Drive, Singapore 637551, Singapore*

† Electronic supplementary information (ESI) available. See DOI: 10.1039/c6sc01829g

limited real efficacy in clinical settings due to collateral damage to non-cancer cells, lower than 100% uptake by the target cancer cells and an overly complicated multi-stage process. Non-viral DNA nanostructures have instead shown some degree of success in the delivery of other molecular cargo like siRNA,[6,7] aptamers,[26–28] and proteins,[29,30] into cells. While the mechanisms are unclear, DNA nanostructures showed the potential to protect their cargo[11] in harsh degradative conditions. Coupled with their natural biocompatible characteristics, DNA nanostructures are well poised to be multi-scenario, programmable and powerful tools for miRNA delivery. We further reasoned that if we can protect the introduced miRNA for a sufficiently long time for its effect to be exerted, we might be able to remove this bottleneck holding back the broad clinical use of therapeutic miRNAs. We designed and assembled a DNA nanostructure bearing the shape of a "Shuriken". We further reasoned that the shuriken's multi-pronged configuration would increase the residence time for robust uptake by cells without any transfection agents. More importantly, the hybridization of miRNA to the complementary DNA segment brings the miRNA to within less than 5 nm of the DNA crossover segment and the triad arms of the shuriken (Fig. 1a). The close proximity provided steric shielding from degradative RNase enzymes. In this paper, we not only showed this steric hindrance DNA-nanostructure conferred protection but also the rest of the expected chain of events from successful delivery to protection and finally effective inhibition of cancer growth of otherwise highly proliferative colorectal cancer cells *in vitro* and in three dimensional (3D) cell culture systems.

Results and discussion

The DNA shuriken was designed based on a DNA star motif (Fig. 1a).[31,32] Briefly, the DNA star motif consisted of one long central strand L (blue), three copies of edge strands M (green) and three copies of peripheral strands S (black). Strand S contained a piece of a DNA sequence (17 bases) that could hybridize to miR-145 5p (23 bases) and protrude out as an overhang. The DNA star motifs then hybridized with three copies of miR-145 to form a DNA shuriken. A toehold 6 bases long is left on the end of the DNA and RNA hybrid duplex to prevent strand displacement. Each arm of the DNA star motif is approximately 10 nm long, while the length of the hybrid duplex overhang is approximately 6 nm. Note that the three arms of the DNA shuriken are not necessarily always in the same plane. The three arms and overhangs are deliberately designed to be very flexible to maximize the contact area and minimize the interaction enthalpy with the cell membrane to further drive its cellular uptake. The outcome of this design is exactly similar to the concept of a "ninja shuriken" rotating, striking a surface and embedding itself on the surface. This embedding theoretically increases the residence time for successful uptake.

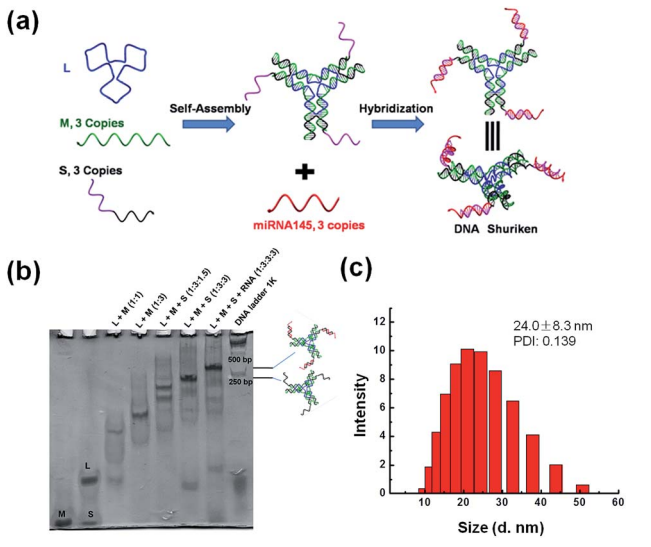

Fig. 1 Design and characterization of the DNA shuriken. (a) A schematic illustration of the DNA shuriken design. The DNA shuriken is a DNA star motif carrying 3 miR-145 strands. (b) Native PAGE analysis of the DNA shuriken. (c) DLS characterization of the DNA shuriken.

Native PAGE was utilized to characterize the formation of the DNA shuriken. As shown in Fig. 1b, both the DNA star motif and the DNA shuriken formed a sharp, dominant band with corresponding expected mobility differences in the gel. The band position of the DNA shuriken is higher than that of the DNA star motif because of the three identical miR-145 cargoes, and the size of the DNA shuriken (205 bp) is comparable to that of the DNA ladder. Dynamic light scattering results (Fig. 1c) further confirmed the formation of the DNA shuriken. The DNA shuriken has an average hydrodynamic diameter of 24.0 ± 8.3 nm, which is consistent with the theoretical value of the design (Fig. S1†).

DNA nanostructures have been proven to be readily taken up by cells[33] without any transfection agents. In this study, we thoroughly investigated the cellular uptake of the DNA shuriken and the effectiveness of this delivery system. Fig. 2a(i and ii) shows the confocal fluorescence image and the cross-sectional view of the cells respectively treated with DNA shuriken for 2 hours. Internalization of the DNA shuriken particles tagged with Cy3 by DLD-1 cells was observed. We also observed that substantial naked miR-145 was internalized by the cells (Fig. 2a(iii and iv)), similar to another report.[33] The time needed for cells to internalize sufficient amounts of DNA shuriken is very important when it comes to its therapeutic efficacy. It was reported that the cellular uptake of DNA origami structures with a size of dozens of nanometers requires more than 12 hours,[3,34] while smaller DNA structures (<20 nm) need 2 to 6 hours.[7,33] In our study, the uptake process is therefore comparatively very fast. Our microplate quantification shows that the relative fluorescence intensities reached a maximum of around three fold higher compared to that of the control within a brief 30 min incubation (Fig. S2†). The observed punctate staining of DNA shuriken–miR-145 (Fig. 2a(i and ii)) suggested endosomal localization of our constructs instead of random dispersion in the cytosol. Thus, we did a colocalization study of DNA shuriken and lysosomes with an incubation time of 2 hours. Most of the internalized DNA shuriken resided in the lysosomes, as indicated by the fluorescent images in Fig. 2b. Statistical analysis also showed that about 80% of the DNA shuriken particles were

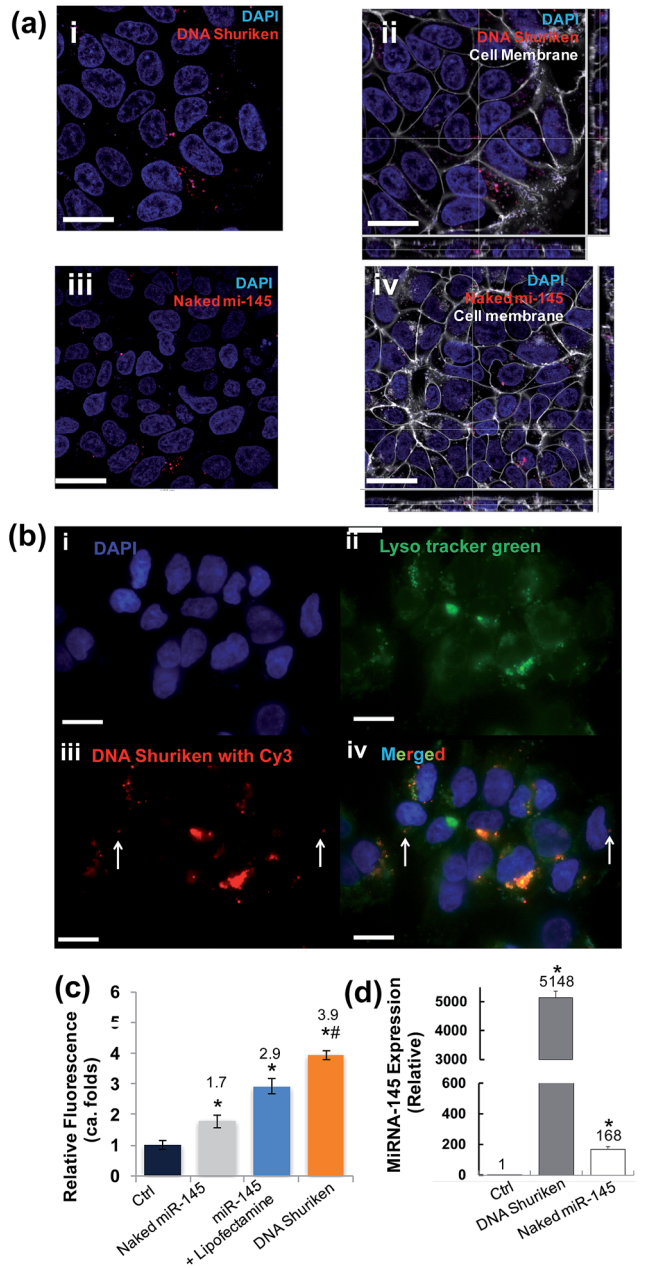

Fig. 2 Internalization of DNA shuriken into cells. (a) Cells were incubated with DNA shuriken–miR-145 or naked miR-145 for two hours before imaging. Cell nuclei were stained with DAPI; miR-145 was tagged with Cy3. (a(i)) Cellular uptake of DNA shuriken–miR145. (a(ii)) The sectioning analysis of DNA shuriken–miR-145 treated cells showed intracellular presence but it was outside of the nucleus. (a(iii)) Comparatively lower cellular uptake of naked miR-145. (a(iv)) The sectional analysis of intracellular localization. (b) Colocalization study of DNA shuriken and lysosomes. Cells were stained with DAPI (b(i)) and Lyso tracker green (b(ii)). Most of the DNA shuriken particles (b(iii), tagged with Cy3) colocalized with lysosomes, and only a few DNA shuriken existed in the cytoplasm, indicated with arrows (b(iv)). (c) Quantification analysis of naked miR-145, miR-145 lipoplex (miR-145 + Lipofectamine) and DNA shuriken (with miR-145) using a microplate reader. The fluorescence signal is normalized to cell numbers and the untreated control. Data represent the mean ± SD, $n = 3$. Student's t-test, $p < 0.05$. *Significantly different from the control group (control). #Significantly different from the Lipofectamine treatment group. A complete data set can be found in Fig. S3.† (d) RT-qPCR quantification of the miR-145 level of DLD-1 cells after 24 hours' treatment. *Let-7a* was used as an internal control. The concentrations of DNA shuriken and naked miR-145 were kept at 200 nM (each DNA shuriken bears three copies of miR-145) and 600 nM respectively in all experiments. Data represent the mean ± SD, $n = 3$. Student's t-test, $p < 0.05$. *Significantly different from the control. Cell membranes were stained and are indicated in white. Scale bar: 20 μm.

trapped in endosomes or lysosomes. To gauge the DNA shuriken performance as a miRNA delivery vehicle, we conducted a comparative study against the common transfection agent, Lipofectamine 2000. Our comparative study shows that the DNA shuriken significantly improved the miRNA-145 delivery as well. We detected close to 2-fold improvement in the DNA shuriken performance when compared to utilizing the Lipofectamine 2000 (Fig. 2c and S3†). To test the versatility of our DNA shuriken platform, we expanded our comparative study to other cell lines. Breast cancer cells, MCF-7, readily took up significant amounts of DNA shuriken particles while in contrast, HMVEC endothelial cells did not (Fig. S3†). In order to further examine the effectiveness of the DNA shuriken platform, we directly quantified the intracellular delivered miR-145 levels with quantitative reverse transcription PCR (RT-qPCR). It was previously reported that different DNA nanostructures can resist enzymatic DNA degradation and stay intact for 4 to 24 hours.[33,34]

Along the same lines, it is therefore believed that this relative stability of DNA nanostructures in physiological conditions can help keep the cargo, single stranded DNA or RNA, safe from enzymatic digestion. Herein, RT-qPCR quantification showed that the miR-145 level is more than 5000 times higher than that of the untreated control even after a long 24 hours in a "foreign-nucleic-acid" unfriendly environment like the cell (Fig. 2d). In contrast, the intracellular level of naked miR-145 treated cells is approximately 30 fold lower than the DNA shuriken counterpart over the same time period of incubation. Our findings clearly show that the designed DNA shuriken can effectively deliver the miR-145 into cells, and stabilize and subsequently release the cargo.

We further investigated the anti-cancer effects of DNA shuriken on the highly proliferative colorectal cancer cell line DLD-1 which does not normally express significant amounts of miR-145. Since uncontrolled cell proliferation is a hallmark of cancer, we therefore employed a flow cytometry-based Ki67 cell proliferation assay to evaluate the therapeutic effect of miR-145. Ki67 is a potent cellular marker for proliferation.[35] As can be seen in Fig. 3a, the percentage of proliferating cells (Ki67 positive) is 77.8%, 85.9% and 81.2% for negative control, the naked miR-145 strand and DNA star motif treated cells, respectively. Strikingly, a significant decrease in the percentage of proliferating cells (*i.e.* 46.3%) was observed for the cells that were treated with the DNA shuriken. It is noteworthy that the anti-proliferative effects of the DNA shuriken are even higher (approximately 1.4 folds) than those of the cells that are cultured in serum free medium devoid of any growth factors (without miR-145 or DNA shuriken treatment). The excellent cell proliferation suppression effect of miR-145 seen here is consistent with another study which directly overexpressed

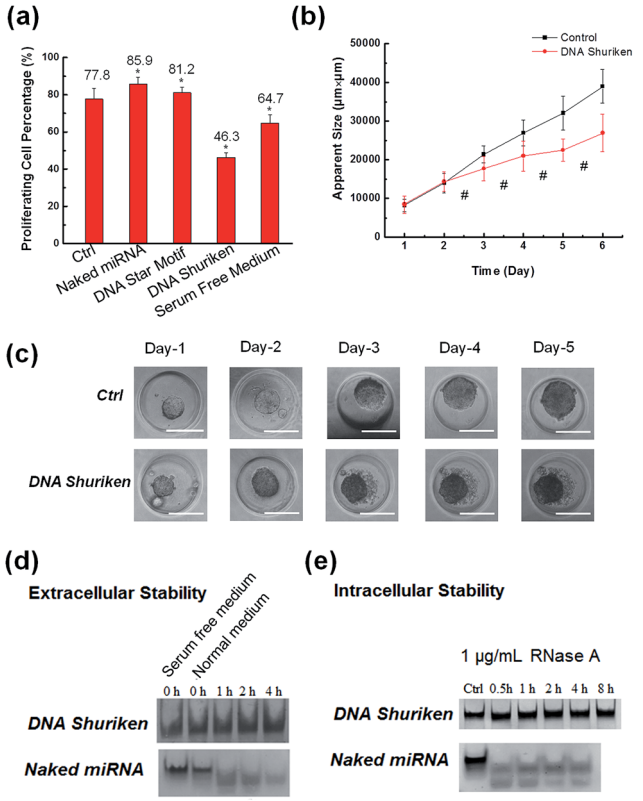

Fig. 3 The therapeutic effect and the stability of DNA shuriken in cell proliferation and 3D tumor growth. (a) Cell proliferation analysis of the DNA shuriken treated cells. (b) Impact of DNA shuriken treatment on tumor size over different time periods. The growth of tumors was assessed by apparent size change. Tumors were treated with DNA shuriken at a final concentration of 200 nM. (c) The effect of DNA shuriken on the tumor spheroid morphology. (d) Extracellular stability of DNA shuriken and naked miR-145. (e) RNase A degradative enzyme assay was employed to represent the efficient miRNA degradative process found in the intracellular environment. Scale bar: 200 μm. Data represent the mean ± SD, $n = 3$. Student's t-test compared to control, $^{*}p < 0.05$, Bonferroni test compared to control, $^{\#}p < 0.001$.

miR-145 from within the cell itself.[36] Our results demonstrated that DNA nanostructures are suitable and effective for delivering external synthetic miR-145 and maintaining efficacy similar to endogenous expressed miR-145. To further the therapeutic effect of the DNA nanostructure platform on a more tumor-like format, we set up a 3D spheroid tumor model based on DLD-1 cells using a micropatterned hydrogel platform.[37,38] The tumors were formed and treated with or without DNA shuriken for 5 days. Then we did a size change with time course analysis on the spheroids (Fig. 3b). After only two days there was a pronounced size difference, and the DNA shuriken treated tumor was 31% smaller (apparent size) than the untreated tumor. Fig. 3c shows the gross morphological evaluation of representative tumor spheroids. For the untreated group, the spheroids grew very fast and had a smooth surface of robust and uniform cell growth, while the DNA shuriken treated tumors were significantly smaller and had many cells "flaking off" from the outer surface. The reduced tumor size and morphology change paralleled the DNA shuriken-mediated anti-proliferative effects on 2D culture plastic growth and further demonstrated the efficacy to curb tumor growth in 3 dimensions. These results clearly showed that DNA shuriken can be an effective and powerful platform for miRNA therapeutics.

To the best of our knowledge, our current work is the first report that uses miRNA loaded DNA nanostructures for miRNA targeted cancer therapy. Although several reports showed that DNA nanostructures carrying siRNA[6,7] or peptides[8,9] had been successfully delivered into cells and taken effect, the details, such as the extracellular and intracellular stability of the DNA nanostructures, cellular uptake mechanisms, and the endosomal escape and cargo release, still remain largely unclear. Thus, elucidating such issues based on current DNA shuriken design is crucial for the future design of more effective, targeted and sophisticated therapeutic DNA nanostructure platforms. Firstly, we investigated the stability of DNA shuriken both in extracellular and intracellular environments (Fig. 3d and e). PAGE gel showed that the DNA shuriken structure was intact in the cell medium for up to 4 hours, whereas naked miR-145 was degraded within one hour. Secondly, to test the protective effect of DNA shuriken inside cells, we subjected the construct to a realistic estimated concentration of intracellular RNase A (1 μg mL^{-1}). Fig. 3e shows that the DNA shuriken was stable for at least 8 hours, and naked miR-145 (unprotected) was quickly broken into two (or more) small fragments in a comparatively short time of 30 min. This reinforces our design strategy of steric hindrance conferred protection of the miRNA cargo. This result is also supported by the much higher measurable intracellular miR-145 level even after 24 hours in Fig. 2d.

This stability is important considering that the majority of our DNA shuriken was entrapped in lysosomes (Fig. 2b). While the mechanism of the lysosomal escape of the miR-145 was not delved into in this study, it did not contradict our findings that the miR-145 complexed in DNA shuriken was able to still exert its anti-cancer bioactivity (Fig. 3a–c). Even in the worst case scenario of being in the lysosomes for 24 hours (Fig. 2b), the all important sequence specificity of miR-145 was not compromised (the qPCR assay is extremely sensitive to sequence specificity changes (Fig. 2d)). Thus, this demonstrated the protective anti-degradative power of DNA shuriken in ensuring the safe passage of miR-145 from cell entry to successfully exerting its bioactivity (Fig. 3).

The non-toxic DNA nanostructures with their powerful structural control and precise spatial functionalization may launch the new era of delivery tools. Future design of DNA nanostructure based drugs emphasizing avoidance of endosome entrapment, customizable intracellular transportation,[25] targeted delivery,[39,40] and tracking of these DNA nanostructures in the cell would further improve the efficacy of this novel DNA nanotechnology.

Conclusions

In summary, we have designed and synthesized a DNA shuriken structure that contains miR-145 as a therapeutic agent against cancer. Its multi-pronged configuration helped with increasing the residence time for robust uptake by cells without any

transfection agents. After entering the cell, the nanostructure continues to protect the miR-145 cargo to greatly suppress cancer cell proliferation and tumor growth. The significant therapeutic effect against cancer was attributed to the protection of the DNA nanostructure carrier as shown in both simulated extracellular and real intracellular environments. Our work showed that DNA nanostructures can be excellent customizable platforms for miRNA based cancer therapies, and have great potential to be expanded to other bioapplications, such as *in vivo* biosensing and bioimaging with specific targeting capability if necessary.[41–44]

Acknowledgements

This work is supported by the Faculty of Engineering-Cross Faculty Grant (R-279-000-414-112).

Notes and references

1 V. Bagalkot, O. C. Farokhzad, R. Langer and S. Jon, *Angew. Chem., Int. Ed.*, 2006, **45**, 8149–8152.
2 Q. Zhang, Q. Jiang, N. Li, L. Dai, Q. Liu, L. Song, J. Wang, Y. Li, J. Tian, B. Q. Ding and Y. Du, *ACS Nano*, 2014, **8**, 6633–6643.
3 Q. Jiang, C. Song, J. Nangreave, X. W. Liu, L. Lin, D. L. Qiu, Z. G. Wang, G. Z. Zou, X. J. Liang, H. Yan and B. Q. Ding, *J. Am. Chem. Soc.*, 2012, **134**, 13396–13403.
4 Y. X. Zhao, A. Shaw, X. H. Zeng, E. Benson, A. M. Nystrom and B. Hogberg, *ACS Nano*, 2012, **6**, 8684–8691.
5 J. Li, C. Fan, H. Pei, J. Shi and Q. Huang, *Adv. Mater.*, 2013, **25**, 4386–4396.
6 H. Lee, A. K. R. Lytton-Jean, Y. Chen, K. T. Love, A. I. Park, E. D. Karagiannis, A. Sehgal, W. Querbes, C. S. Zurenko, M. Jayaraman, C. G. Peng, K. Charisse, A. Borodovsky, M. Manoharan, J. S. Donahoe, J. Truelove, M. Nahrendorf, R. Langer and D. G. Anderson, *Nat. Nanotechnol.*, 2012, **7**, 389–393.
7 Z. You, H. Qian, C. Z. Wang, B. F. He, J. W. Yan, C. Mao and G. S. Wang, *Biomaterials*, 2015, **67**, 137–150.
8 J. Li, H. Pei, B. Zhu, L. Liang, M. Wei, Y. He, N. Chen, D. Li, Q. Huang and C. Fan, *ACS Nano*, 2011, **5**, 8783–8789.
9 V. J. Schuller, S. Heidegger, N. Sandholzer, P. C. Nickels, N. A. Suhartha, S. Endres, C. Bourquin and T. Liedl, *ACS Nano*, 2011, **5**, 9696–9702.
10 S. Surana, J. M. Bhat, S. P. Koushika and Y. Krishnan, *Nat. Commun.*, 2011, **2**, 340.
11 C. Y. Tay, L. Yuan and D. T. Leong, *ACS Nano*, 2015, **9**, 5609–5617.
12 M. I. Setyawati, R. V. Kutty, C. Y. Tay, X. Yuan, J. Xie and D. T. Leong, *ACS Appl. Mater. Interfaces*, 2014, **6**, 21822–21831.
13 M. Giovanni, M. I. Setyawati, C. Y. Tay, W. S. Kuan and D. T. Leong, *Adv. Funct. Mater.*, 2015, **25**, 3840–3846.
14 D. S. Lee, H. Qian, C. Y. Tay and D. T. Leong, *Chem. Soc. Rev.*, 2016, **45**, 4199–4225.
15 V. Ambros, *Nature*, 2004, **431**, 350–355.
16 D. P. Bartel, *Cell*, 2009, **136**, 215–233.
17 M. Sachdeva and Y. Y. Mo, *Am. J. Transl. Res.*, 2010, **2**, 170–180.
18 M. Fuse, N. Nohata, S. Kojima, S. Sakamoto, T. Chiyomaru, K. Kawakami, H. Enokida, M. Nakagawa, Y. Naya, T. Ichikawa and N. Seki, *Int. J. Oncol.*, 2011, **38**, 1093–1101.
19 B. Dalby, S. Cates, A. Harris, E. C. Ohki, M. L. Tilkins, P. J. Price and V. C. Ciccarone, *Methods*, 2004, **33**, 95–103.
20 A. Sharei, J. Zoldan, A. Adamo, W. Y. Sim, N. Cho, E. Jackson, S. Mao, S. Schneider, M. J. Han, A. Lytton-Jean, P. A. Basto, S. Jhunjhunwala, J. Lee, D. A. Heller, J. W. Kang, G. C. Hartoularos, K. S. Kim, D. G. Anderson, R. Langer and K. F. Jensen, *Proc. Natl. Acad. Sci. U. S. A.*, 2013, **110**, 2082–2087.
21 A. K. Chen, M. A. Behlke and A. Tsourkas, *Nucleic Acids Res.*, 2008, **36**, 69.
22 P. J. Santangelo, B. Nix, A. Tsourkas and G. Bao, *Nucleic Acids Res.*, 2004, **32**, 57.
23 C. D. Medley, T. J. Drake, J. M. Tomasini, R. J. Rogers and W. Tan, *Anal. Chem.*, 2005, **77**, 4713–4718.
24 Q. Wang, H. Cheng, H. Peng, H. Zhou, P. Y. Li and R. Langer, *Adv. Drug Delivery Rev.*, 2015, **91**, 125–140.
25 L. Liang, J. Li, Q. Huang, J. Shi, H. Yan and C. H. Fan, *Angew. Chem., Int. Ed.*, 2014, **53**, 7745–7750.
26 C. Wu, D. Han, T. Chen, L. Peng, G. Zhu, M. You, L. Qiu, K. Sefah, X. Zhang and W. Tan, *J. Am. Chem. Soc.*, 2013, **135**, 18644–18650.
27 P. Charoenphol and H. Bermudez, *Mol. Pharmaceutics*, 2014, **11**, 1721–1725.
28 R. Mo, T. Jiang, W. Sun and Z. Gu, *Biomaterials*, 2015, **50**, 67–74.
29 X. Liu, Y. Xu, T. Yu, C. Clifford, Y. Liu, H. Yan and Y. Chang, *Nano Lett.*, 2012, **12**, 4254–4259.
30 S. M. Douglas, I. Bachelet and G. M. Church, *Science*, 2012, **335**, 831–834.
31 Y. He, T. Ye, M. Su, C. Zhang, A. E. Ribbe, W. Jiang and C. Mao, *Nature*, 2008, **452**, 198–201.
32 H. Qian, C. Tian, J. Yu, F. Guo, M. S. Zheng, W. Jiang, Q. F. Dong and C. Mao, *Small*, 2014, **10**, 855–858.
33 A. S. Walsh, H. Yin, C. M. Erben, M. J. Wood and A. J. Turberfield, *ACS Nano*, 2011, **5**, 5427–5432.
34 C. E. Castro, F. Kilchherr, D. Kim, E. L. Shiao, T. Wauer, P. Wortmann, M. Bathe and H. Dietz, *Nat. Methods*, 2011, **8**, 221–229.
35 T. Scholzen and J. Gerdes, *J. Cell. Physiol.*, 2000, **182**, 311–322.
36 H. Zhu, U. Dougherty, V. Robinson, R. Mustafi, J. Pekow, S. Kupfer, Y. C. Li, J. Hart, K. Goss, A. Fichera, L. Joseph and M. Bissonnette, *Mol. Cancer Res.*, 2011, **9**, 960–975.
37 S. L. Chia, C. Y. Tay, M. I. Setyawati and D. T. Leong, *Small*, 2015, **11**, 702–712.
38 C. Y. Tay, M. S. Muthu, S. L. Chia, K. T. Nguyen, S. S. Feng and D. T. Leong, *Adv. Funct. Mater.*, 2016, **26**, 4046–4065.
39 K. Ma, D. D. Wang, Y. Lin, J. Wang, V. Petrenko and C. Mao, *Adv. Funct. Mater.*, 2013, **23**, 1172–1181.
40 N. K. Niu, J. J. Yin, Y. X. Yang, Z. L. Wang, Z. W. Zhou, Z. X. He, X. W. Chen, X. J. Zhang, W. Duan, T. X. Yang and S. F. Zhou, *Drug Des., Dev. Ther.*, 2015, **9**, 4441.

41 C. Li, F. Li, Y. Zhang, W. Zhang, X. E. Zhang and Q. Wang, *ACS Nano*, 2015, **9**, 12255–12263.
42 C. Li, L. Cao, Y. Zhang, P. Yi, M. Wang, B. Tan, Z. Deng, D. Wu and Q. Wang, *Small*, 2015, **11**, 4517–4525.
43 J. Li, P. Cai, A. Shalviri, J. T. Henderson, C. S. He, W. D. Foltz, P. Prasad, P. M. Brodersen, Y. H. Chen, R. DaCosta, A. M. Rauth and X. Y. Wu, *ACS Nano*, 2014, **8**, 9925–9940.
44 M. I. Setyawati, R. V. Kutty and D. T. Leong, *Small*, 2016, DOI: 10.1002/smll.201601669.